LA-UR-22-28005

Approved for public release; distribution is unlimited.

Title:	LANL Activities on Mechanistic Approach to Analyzing and Improving Unconventional Hydrocarbon Production
Author(s):	Viswanathan, Hari S. Carey, James William Xu, Hongwu Karra, Satish
Intended for:	Report
Issued:	2022-08-03

LANL Activities on Mechanistic Approach to Analyzing and Improving Unconventional Hydrocarbon Production

WORK PERFORMED UNDER AGREEMENT

FWP-FE406-408-409

Final Report

PRINCIPAL INVESTIGATORS

Bill Carey: 505-667-5540, bcarey@lanl.gov Satish Karra: 505-606-1894, satkarra@lanl.gov Hongwu Xu: 505-665-9266, hxu@lanl.gov Qinjun Kang: 505-665-9663, qkang@lanl.gov

PROJECT LEADER

Hari Viswanathan: 505 665 6737, viswana@lanl.gov

SUBMITTED TO

U. S. Department of Energy National Energy Technology Laboratory

7 July 2022

Abstract

Hydrocarbon production from shale reservoirs is inherently inefficient and challenging since these are low permeability plays. In addition, there is a limited understanding of the fundamentals and the controlling mechanisms, further complicating how to optimize these plays. Herein, we summarize our experimental and computational efforts fully and partially supported by the fundamental shale portfolio to reveal unconventional shale fundamentals and devise development strategies to enhance extraction efficiency with a minimal environmental footprint. Integrating these fundamentals with machine learning, we outline a pathway to improve the predictive power of our models, which enhances the forecast quality of production, thereby improving the economics of operations in unconventional reservoirs. For instance, we have developed science-informed workflows and platforms for optimizing pressure-drawdown at a site, which allow operators to make reservoir-management decisions that optimize recovery in consideration of future production. Recently, our work relies on the hybridization of physics-based prediction and machine learning, whereby accurate synthetic data (combined with available site data) can enable the application of machine learning methods for rapid forecasting and optimization. Consequently, the workflow and platform are readily extendable to operations at other sites, plays, and basins.

1. Introduction

Shale reservoirs have redefined the energy landscape of the world (Melikoglu, 2014). Shale reservoirs currently contribute to 70% of U.S. natural gas production and 60% of U.S. oil production (Perrin & Geary, 2019). However, these reservoirs possess unique characteristics that entail custom-designed development plans (Mehana & El-monier, 2016). Currently, we recover less than 10% of the hydrocarbons in place from these low permeability plays with the most efficient development plan (Alharthy et al., 2015). This low efficiency is also due to the limited understanding of how shale properties effect hydrocarbon transport through porous and fractured media. Therefore, a fundamental understanding and quantification of these effects are required for devising better development plans to improve the current recovery factors (Middleton et al., 2017).

Shale reservoirs are governed by physical processes that differ from those that dominate conventional reservoirs (Sondergeld et al., 2010). Whereas porous flow dominates the latter and are described adequately by Darcy's law, the former is dominated by flow in fractures and diffusion in the tight matrix that cannot be simply described by Darcy's law (Hyman et al., 2015). Consequently, the strategies and tools honed over decades for conventional reservoirs do not readily transfer to unconventional reservoirs, inhibiting the ability to optimize reservoir management and, hence, to maximize recovery (Mehana et al., 2021a; Mehana et al., 2021b). As a result, shale reservoirs have poor recovery efficiencies (Seales et al., 2017).

The unique characteristics of shale include the abundance of nanopores and the impact of heterogeneous mineralogy (Clarkson et al., 2013; Ross & Bustin, 2009). Nanoconfinement of fluids creates numerous unconventional physicochemical processes (Chen et al., 2015b; O'Malley et al., 2016; Riewchotisakul & Akkutlu, 2015). For instance, confined-fluid phase behavior and properties significantly deviate from bulk behavior (Liu & Zhang, 2019). In addition, adsorption is the primary storage mechanism for hydrocarbons, unlike pore-filling in conventional reservoirs (Ambrose et al., 2010). Notably, the shale matrix, especially organic pores, also experiences a degree of deformation, affecting their productivity (Neil et al., 2020b).

Shale is a fine-grained clastic sedimentary rock composed of a mixture of quartz, clay, and carbonate minerals (Rickman et al., 2008). However, the percentages of these minerals differ among shale plays. For instance, Eagle Ford is a carbonate-rich shale, while Barnett is a quartz-rich play (Chermak & Schreiber, 2014). Apart from the heterogeneous mineral composition, the total organic content (TOC) of shale formations adds a critical degree of complexity to reservoirs characterization (Curtis et al., 2012). Historically, shale organic content is the hydrocarbon *source* for conventional reservoirs and was not viewed as a viable target for *primary* production. Contrary to other minerals, organic matter does not have a definite chemical structure. However, the organic matter's maturity critically determines the organic pore structure and the fluids therein.

The heterogeneous mineral composition and the thermal maturity of shale pores explain the mixed wettability nature of shale. Besides being a critical property for transport, wettability also affects the fluid distribution in the pores. Uniquely, shale formations usually have a complex natural fracture system that plays a significant role in hydraulic fracture operational success.

Shale reservoirs have become a significant energy resource. Nevertheless, they are challenging to develop efficiently because of our current limited understanding of mechanisms controlling production. In this final report, we summarize our main project results and contributions that further our knowledge of shale reservoirs and that develop strategies for optimizing production. Figure 1 shows the organization of our project into three fundamental tasks reflecting differing scales of hydrocarbon from transport from rock to the well: 1) Matrix; 2) Tributary Fracture Zone; and 3) Primary Hydraulic Fractures. We conduct focused research at each of these scales with the objective of developing an integrated approach to optimizing production. The small-scale matrix processes are governed by nano-size pores that are the ultimate source of hydrocarbon. Medium-scale fractures are composed of existing natural fractures and fracture damage zones that create higher permeability pathways and that connect the matrix to the primary hydraulic fractures. Large-scale, high-permeability pathways consist of the propped, primary hydraulic fractures.

Transport time of hydrocarbon from rock to well decreases as the scale shifts from the matrix to the primary hydraulic fractures. This accounts for the rapid decline of production with time shown in Figure 1. Early production is dominated by flow from the large, primary hydraulic fractures. Production in the medium-term is dominated by flow occurring in unpropped, natural fractures and the unpropped, induced fractures surrounding the primary hydraulic fractures. After these have drained, all subsequent hydrocarbon must originate in the matrix which involves slow, diffusive transport or flow via very low permeability paths. We illustrate the spatial organization of these three scales in Figure 2.

The remainder of the report provides a summary of results of for the three primary research areas, reflecting our analysis of production in terms of scale and time. Matrix processes are discussed in Section 2;Tributary Fracture Zone processes are discussed in Section 3; the Primary Hydraulic Fracture system is discussed in Section 4; and a Machine Learning Analysis of Production integrating these results is given in Section 5.

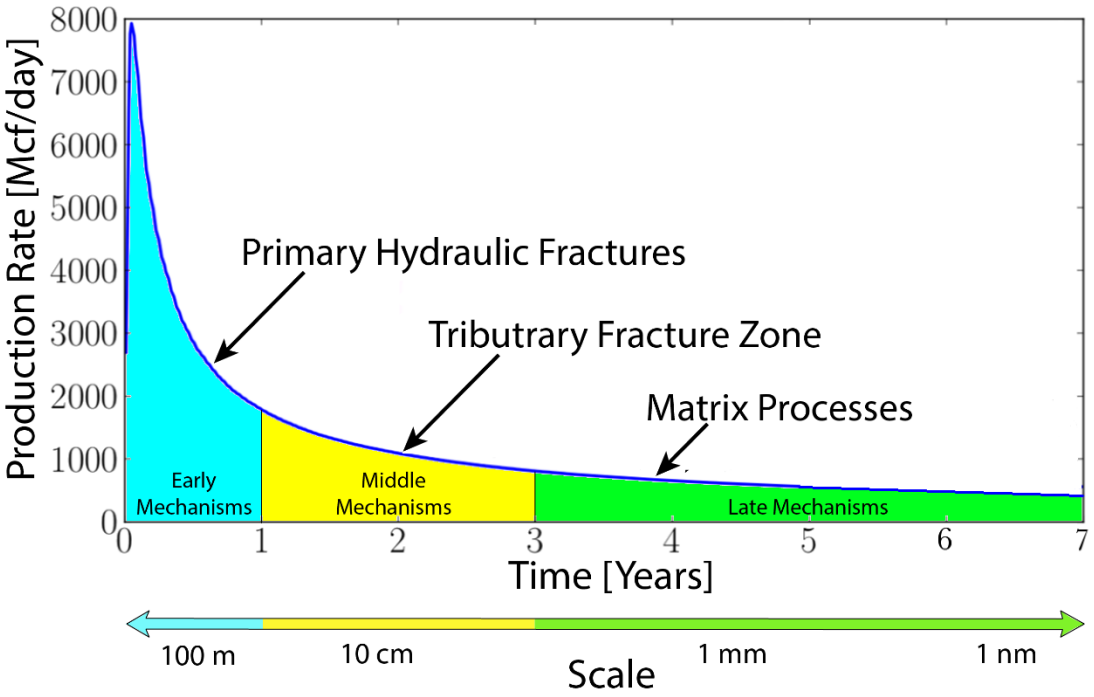

Figure 1. Schematic diagram illustrating the decline of a typical unconventional hydrocarbon production curve as a function of time. The conceptual model for this research project recognizes that production mechanisms change with time with early production derived from large-scale primary hydraulic fractures, medium-scale production derived from smaller-scale fractures connected to the primary hydraulic fractures, and small-scale production derived from the matrix that feeds hydrocarbon to the fractures (also see Figure 2). Project research is organized into efforts focused at each of these scales combined with a scale-integrating analysis to develop methods of optimizing overall hydrocarbon production.

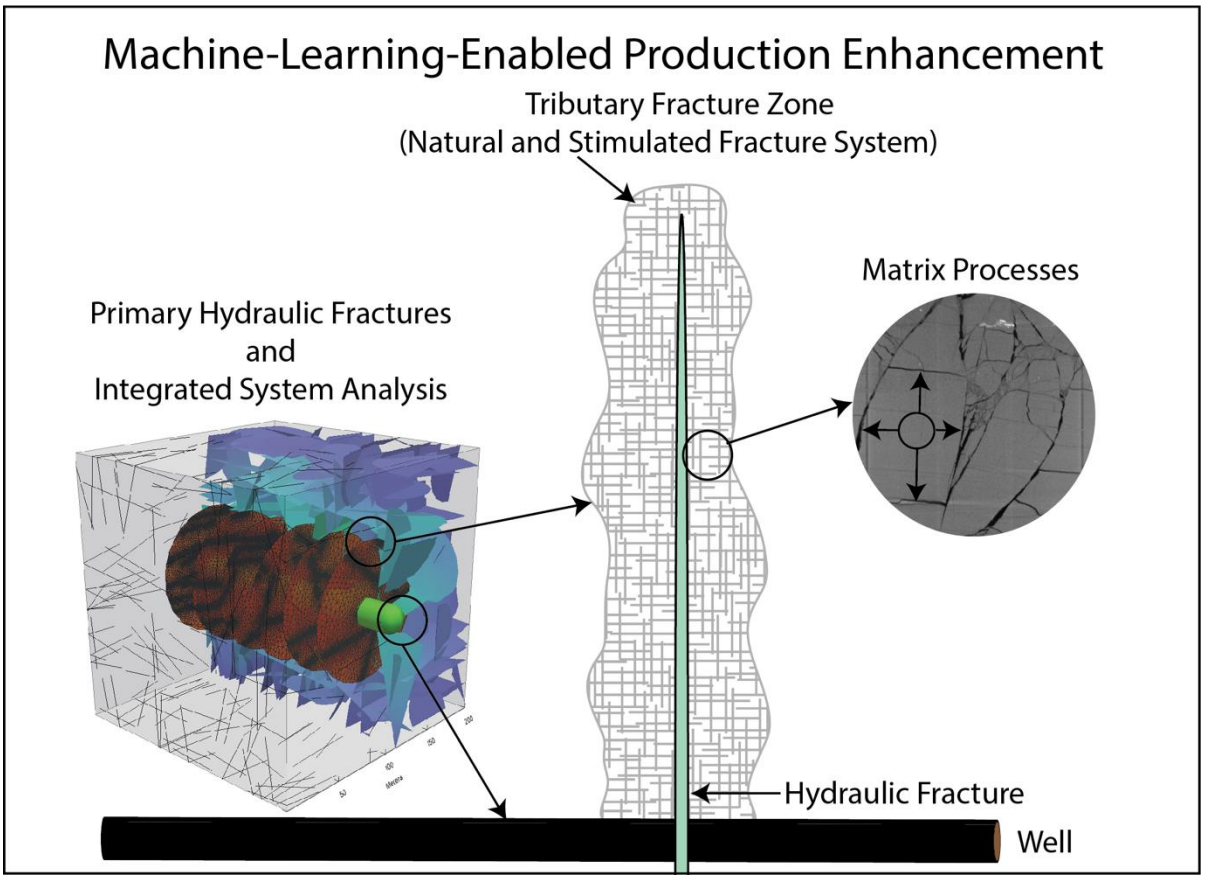

Figure 2. Conceptual model of three distinct scales of hydrocarbon production: small-scale matrix processes that feed into medium-scale tributary fractures that drain into the primary hydraulic fractures.

2. Matrix Processes

Traditionally, shale formations are considered either a source rock or a reservoir seal, mostly because of their ultralow (nanoDarcy) permeability and the abundance of nanopores. Effective development of these formations as hydrocarbon reservoirs necessitates a fundamental understanding of the anomalous phenomena controlling the fluid behavior in the matrix pores. In essence, fluids confined in nanopores behaves differently than larger conventional pores because fluid/solid interactions dominate fluid properties. Under these conditions, traditional continuum assumptions for the fluid phase are usually violated. For example, we have shown that simulating fluid flow through shales with a conventional reservoir simulator leads to inaccurate predictions of key quantities of interest, such as permeability, that can be incorrect by several orders of magnitude (Chen et al., 2015a). Consequently, the standard thermodynamic principles are not applicable at these conditions, which requires development of computer codes that incorporate the physics of confined fluids.

Slippage and adsorption are critical surface phenomena whose effects are magnified under confinement. In Wang et al. (2016), we used the lattice Boltzmann method (LBM) to simulate a homogenous shale matrix considering both slippage and adsorption effects on fluid transport. We observed that the slippage effect is more substantial than the adsorption effect at lower pressures,

leading to higher apparent permeability than intrinsic permeability. On the other hand, the slippage effect is weaker than the adsorption at higher pressures, resulting in apparent permeability lower than intrinsic permeability at higher pressures. In addition, we highlighted the impact of surface and Knudsen diffusion on the apparent permeability as shown in Figure 3. Both surface and Knudsen diffusion contributions to the fluid transport and are magnified at low pressures where the apparent permeability is two orders of magnitude higher. Conversely, these contributions are reduced at higher pressures. In addition, we found that surface diffusion is highly promoted for pores less than 20 nm.

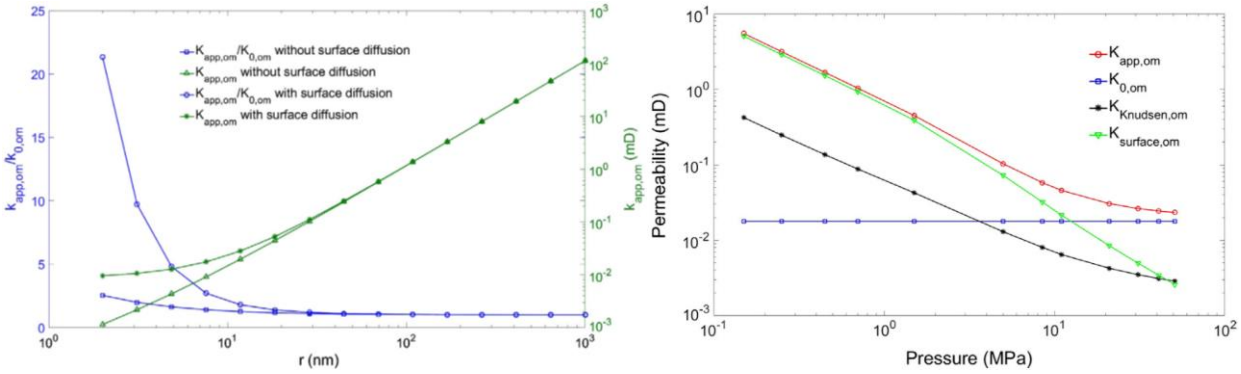

Figure 3. The contribution of surface and Knudsen diffusion to the apparent permeability for different pore radiuses (the left, P_{in} = 22 MPa and P_{out} = 20 MPa) and pressures (the right, The average pore radius, r = 2 nm, and standard deviation = 0.25 nm.) From Wang et al. (2016).

Observation of fluid behavior within the matrix using experimental methods is challenging due to the small size of shale nanopores. Experimental techniques, such as optical microscopy and X-ray/neutron micro-tomographic imaging, lack the necessary resolution to infer structures and properties of nanopores (Yang et al., 2019). Furthermore, although electron microscopic methods can resolve nanoscale features (Yoon & Dewers, 2013), they are challenging to combine with *in situ* environmental cells containing fluids. Recently, our research team at Los Alamos National Lab has made significant inroads to address this problem using small-angle neutron scattering (SANS) combined with an *in situ* pressure cell to provide experimental data over relevant length scales and environmental conditions (Hjelm et al., 2018; Neil et al., 2020a; Neil et al., 2020b). SANS provides *in situ* measurements of the relevant structures and properties of geomaterials, including the unique capability to probe both open and closed pores and pores smaller than the typical probing molecules used for mercury intrusion or gas absorption (Xu, 2020). Employing SANS, the team revealed key new insights into the behavior of pressurized fluid within shale nanopores, including water accessibility differences between clay- and carbonate-rich shale nanopores (Neil et al., 2020a) and trapping of methane gas in shale nanopores due to kerogen deformation (Neil et al., 2020b).

Matrix processes are complex, which necessitates integrating multiple techniques to reveal the main controlling mechanisms. One example was integrating experiments and molecular simulation to quantify the confinement effects on the methane transport in shale pores (Neil et al., 2020a). Neil et al. (2020b) highlighted the significance of pressure management to optimize hydrocarbon recovery. Basically, they found that producing aggressively with large pressure gradients can close off matrix pores entrapping hydrocarbons and reducing production, as shown in Figure 4. In addition, they reported a reduction of the diffusion coefficients under confinement.

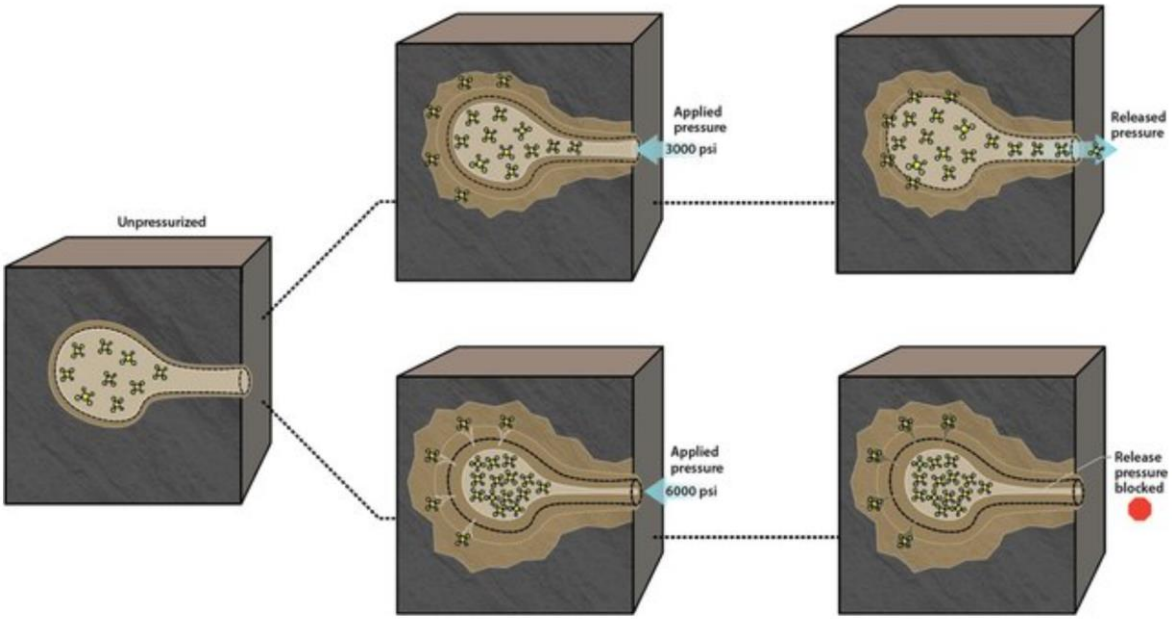

Figure 4. The schematic depicts the pressure cycling on the matrix deformation and fluid retention (Neil et al., 2020a). The methane is injected into the shale samples at a pressure of 3000 psi in the upper branch and is produced at ambient conditions. On the lower branch, the fluid is injected at 6000 psi and produced at ambient conditions. More retention is observed for the high-pressure cycles, mostly because of the collapse of pores in the organic matrix.

3. Tributary Fracture Zone

In our conceptual model, the tributary fracture zone (TFZ) is the connection between the matrix and the primary hydraulic fractures. The primary hydraulic fractures originate from the well and provide propped, high-permeability access to the surrounding shale reservoir. However, the primary fractures by their very nature have contact with a very small fraction of the entire shale reservoir. This problem was recognized by Bažant et al. (2014) who argued that successful hydrocarbon production must involve some form of a dense, interconnected secondary (or in our language, tributary) fracture system that provides the necessary interface with the bulk shale mass. In our work, we have taken two approaches to enhancing production from these unpropped, medium-scale fractures: 1) enhanced fracture branching off of the primary hydraulic fracture and 2) pressure management to avoid closure of the unpropped tributary fracture zone.

Working with collaborators at Northwestern University, we were able to show numerically that weak layers in shale formations could be exploited to enable hydraulic fracture branching, as shown in Figure 5 (Rahimi-Aghdam et al., 2019). We argued that this branching provides the theoretical fracture density in the tributary fracture zone needed to account for observed hydrocarbon recovery and could be used as a basis for enhancing production.

In a recent paper, we completed an experimental study of fracture branching that demonstrated injection and fluid conditions that promote fracture branching (Li et al. 2021a; Figure 6). In this study, we used plaster as an analog material because we needed reproducible material properties and the ability to create pre-existing weakness structures. The results showed that branching can develop as long as there exist weak zones of moderately enhanced permeability in comparison

with the matrix. These weak zones could be bedding planes or pre-existing natural fractures. This work showed that injection rates and hydraulic fluid properties (i.e., viscosity) could be engineered to create fracture branches that should enhance hydrocarbon production.

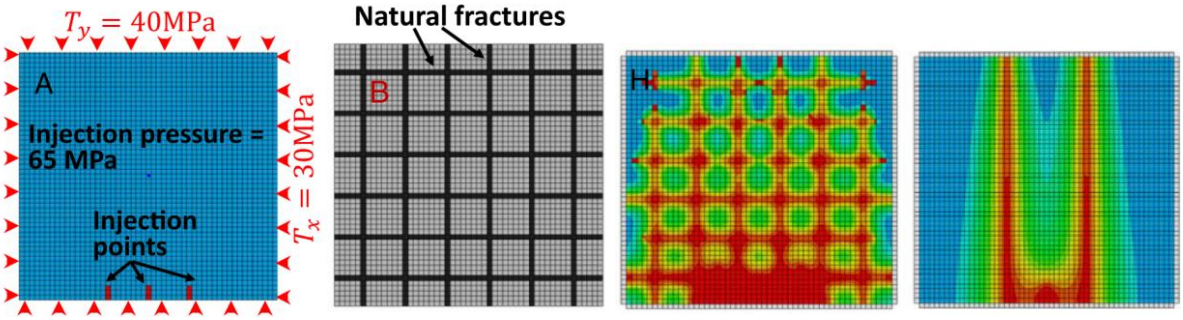

Figure 5. The impact of natural fractures and weak layers on fracture propagation (Rahimi-Aghdam et al., 2019): A) the initial conditions, B) the natural fractures and weak layers distribution, C) the fracture propagation with the presence of weak layers D) the fracture propagation without the weak layers.

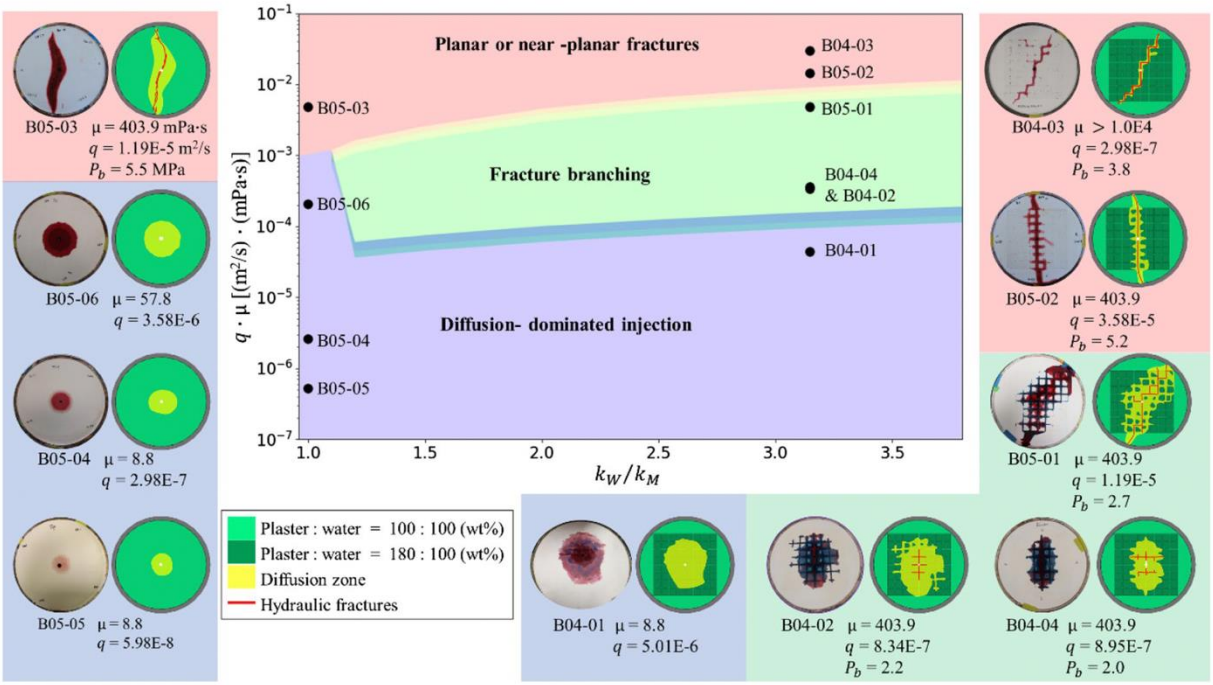

Figure 6. Development of a phase diagram explaining fracture branching (central rectangle) based on experimental results obtained on an analog material. Fracture branching can occur given moderately enhanced permeability of weak natural fractures or bedding planes (k_W) compared with matrix permeability (k_M) combined with an appropriate injection rate (q) and injection fluid viscosity (μ). The images on the border are photographs of hydraulic fracture experiments in fracture that show three kinds of behavior: diffusion-dominated response that not allow formation of hydraulic fractures; classical, simple hydraulic fractures ("planar or near-planar fractures"); and injection conditions promoting fracture branching. From Li et al. (2021a).

In the second approach, we investigated the physical properties of unpropped fractures and their susceptibility to pressure management. Our conceptual model here is that producing hydrocarbon as fast as possible (basically completely opening the valves) results in a decrease in pore pressure that can result in the closure of unpropped fractures. If these fractures in the tributary fracture network are closed, then we shut down an important transport pathway between the matrix and the primary hydraulic fractures. Whether pressure management can affect fracture permeability can be determined by experimental analysis of fracture behavior.

One of the first tasks we accomplished was the development of an experimental capability to examine fracture permeability as a function of stress conditions (Figure 7). Our intent was to study fractures under representative, subsurface conditions. For this, we developed the triaxial direct-shear approach that allowed us to create and maintain fractures at high-pressure and elevated temperature, to measure permeability before, during and after fracture creation and reactivation, and to image fracture properties with x-rays. This experimental system was developed and described in a series of papers: Carey et al. (2015) and Frash et al. (2016, 2017).

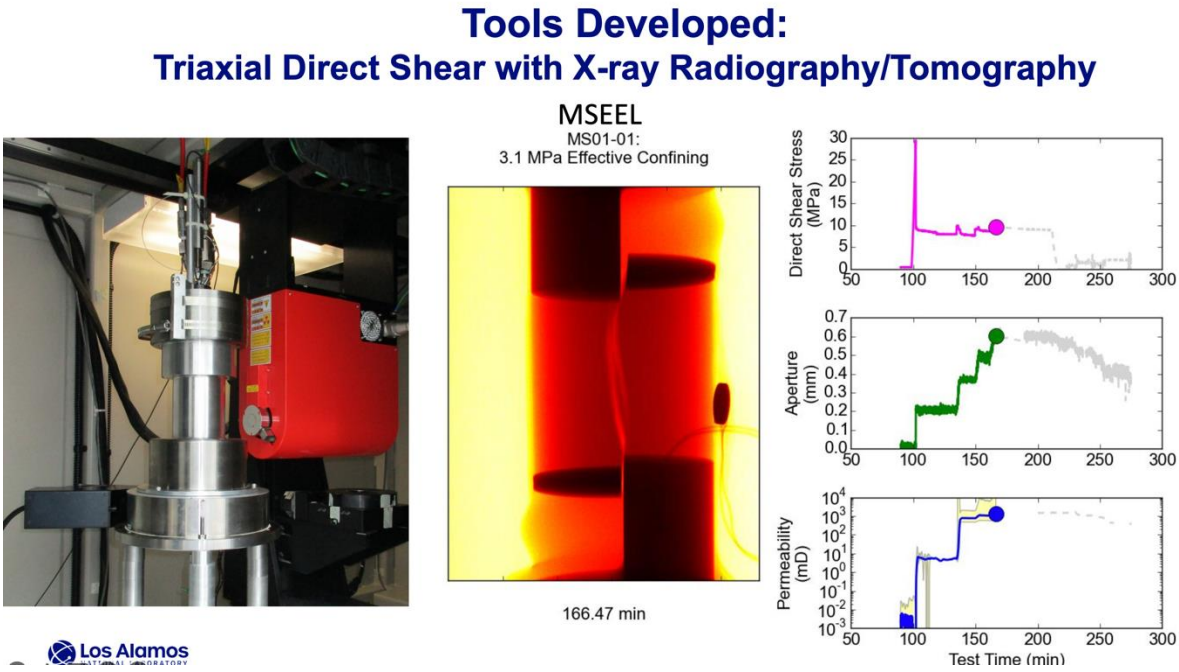

Fig. 7. The triaxial direct-shear system with simultaneous x-ray radiography and tomography. At left is the aluminum coreholder inside an x-ray cabinet with the orange x-ray generating device. In the center is an x-ray radiograph showing a fracture as it formed in the Marcellus shale. At right are data streams including the shear stress, the aperture of the fracture system and the permeability of the fracture system all time-synchronized with the x-ray radiography.

With this new experimental capability, we first investigated the impact of depth on the potential for hydrocarbon production (Figure 8). Utica shale specimens were fractured at progressively greater stress combined with simultaneous measurements of fracture permeability and fracture aperture. The data reveal the progressive loss of fracture permeability with depth (Frash et al. 2017). Although depth is not a property that can be controlled, these measurements do provide a

guide indicating that greater depth can reduce potential hydrocarbon production from the tributary fracture system.

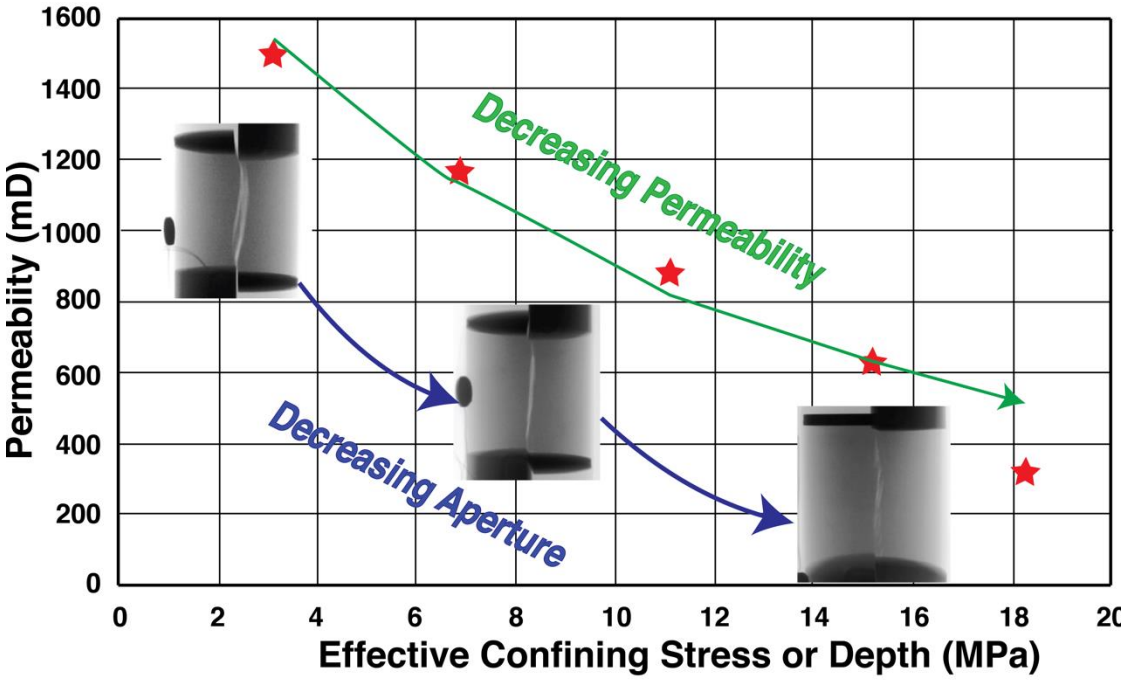

Figure 8. Fracture permeability of Utica shale measured as a function of stress at the time of fracture creation. The x-ray radiographs show the progressive decrease in fracture aperture accompanying the loss of permeability at higher stress (or depth) (Frash et al. 2017).

We next investigated whether controlling the extent of fracture displacement (e.g., by repeated hydraulic stimulation) could be used to manipulate permeability (Figure 9). In these experiments, a specimen of Marcellus shale was fractured at low stress (5 MPa) and then "re-stimulated" by increasing fracture displacement. The hydraulic aperture (and permeability) increased with each displacement. At the final step, the specimen was re-stimulated with a simultaneous increase to 30 MPa confining stress. This resulted in an almost complete loss of permeability and hydrocarbon production potential (Welch et al., 2022). The results show that while displacement can increase hydrocarbon production by enhancing unpropped fracture permeability, this permeability can be lost if they are accompanied by large stress increases as can occur during pressure drawdown.

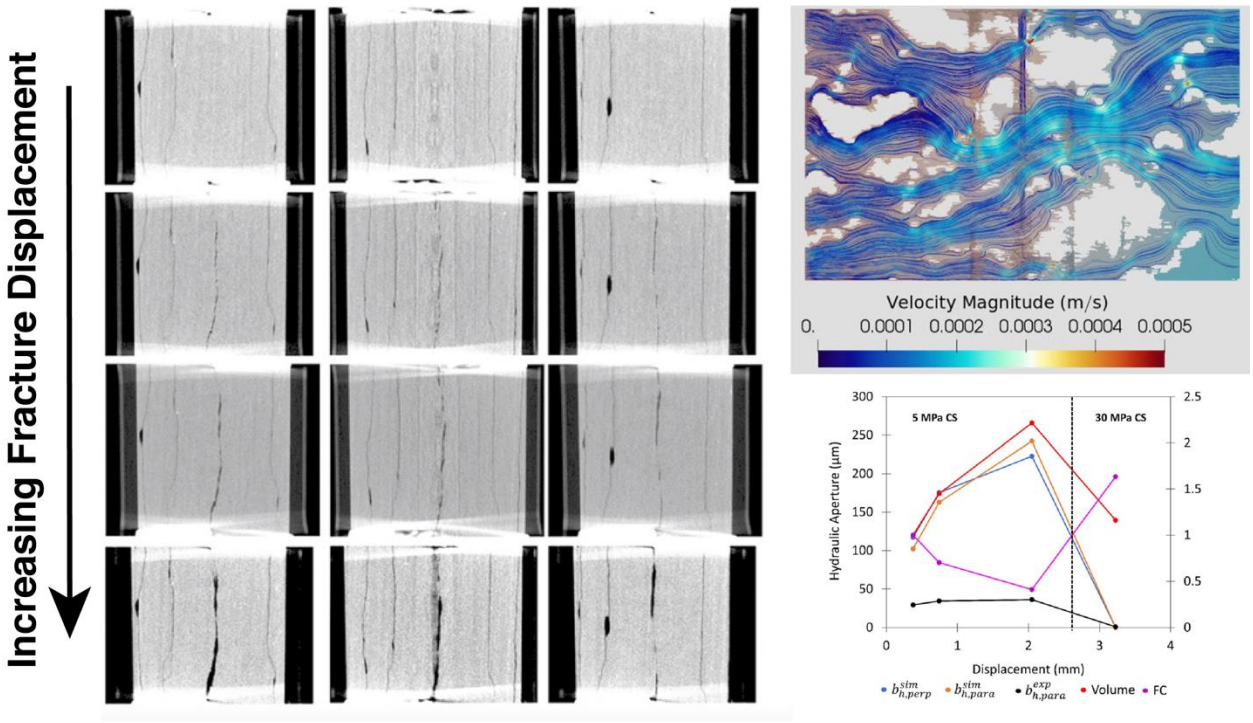

Figure 9. (left) X-ray tomography of a complex Marcellus sample containing natural fractures and an induced shear fracture (central fracture that widens with increasing displacement). (upper right) Computational fluid dynamics simulation of fluid flow paths through the shear fracture showing the profound influence of closed or tight regions on permeability. (lower right) Plot of hydraulic aperture as a function of displacement. Aperture increases with displacement until a combination of increasing displacement with increasing confining stress results in a dramatic loss of permeability. From Welch et al. (2022).

We studied a suite of Marcellus shale specimens obtained from well MIP-3H at the Marcellus Shale Energy and Environment Laboratory (MSEEL). Our objective here was to examine the sensitivity of a variety of Marcellus shale lithologies to pressure drawdown effects (Li et al. 2021b). The results shown in Figure 10 indicate that the hydraulic aperture or permeability of all specimens decreased with increasing pressure drawdown (i.e., increasing effective normal stress). However, the slopes of the lines varied (indicating greater or lesser fracture compliance) and the initial fracture apertures varied greatly. Note that the apertures are plotted on a logarithmic scale such that small changes in value reflect very large changes in fracture permeability.

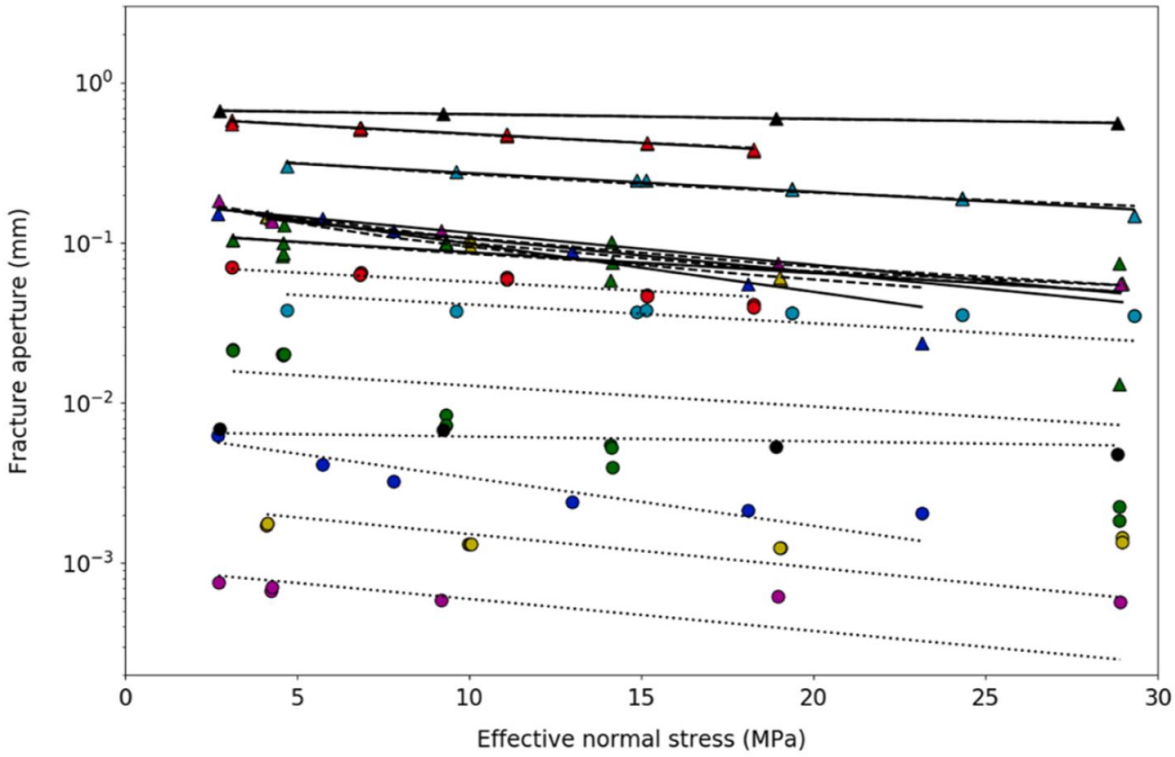

Figure 10. A summary of the impact of changing effective normal stress (equivalent to an analysis of the effects of pressure drawdown) on the hydraulic aperture (or permeability) of seven different Marcellus shale specimens. The triangles are mechanical fracture apertures and the circles are hydraulic apertures color-coded for the same specimens. Increasing pressure drawdown (i.e., higher effective normal stress) decreased both types of apertures. Note that there was a wide variation in initial aperture reflecting differing shale properties. From Li et al. (2021b).

In Li et al. (2021b), we used the results of the Marcellus shale shown in Figure 10 to develop a guide to evaluating the effectiveness of pressure drawdown as a function of shale properties (Figure 11). This plot characterizes shale fractures in terms of fracture compliance, α (a measure of the change in fracture aperture as a function of changes in applied stress) and N, the ratio of hydraulic and mechanical apertures (small N indicates fractures with rough walls and/or significant regions of fracture closure. Using the experimental techniques outlined in Figures 6-10, we can measure α and N and evaluate the susceptibility of a particular lithology to pressure management strategies. Li et al. (2021b) found that some Marcellus shale lithologies were relatively insensitive to pressure management while others had high sensitivity.

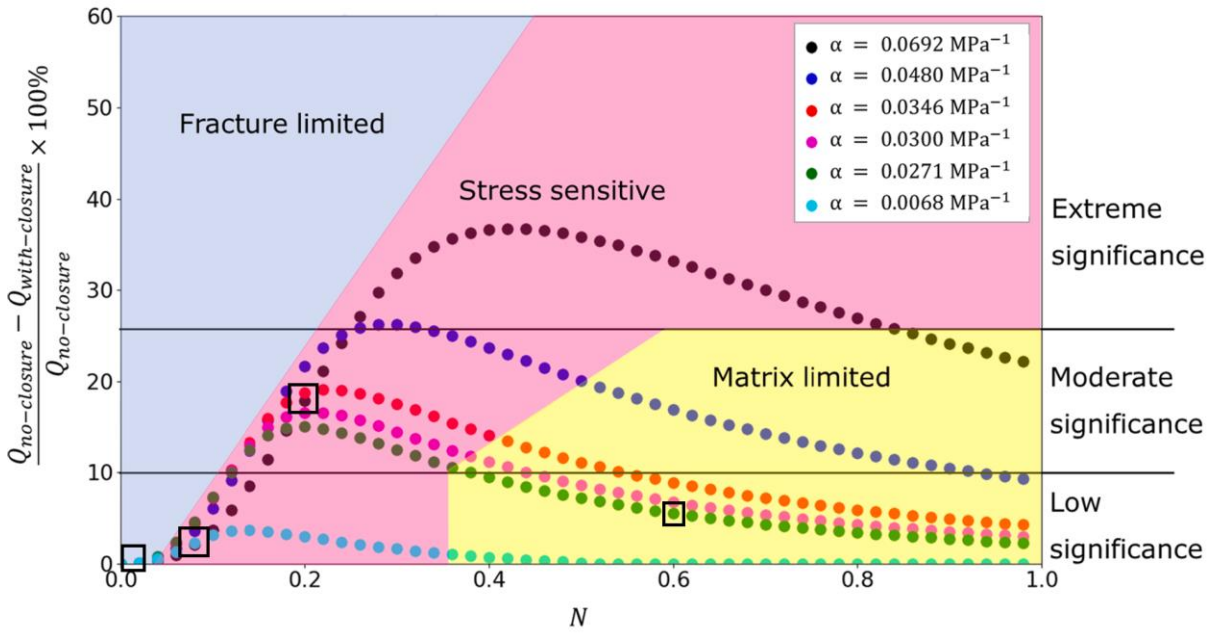

Figure 11. Calculated impacts of pressure drawdown on hydrocarbon production as a function of shale properties. The y-axis is the increase in hydrocarbon production that can be obtained by practicing pressure management. The x-axis is the ratio of hydraulic to mechanical aperture of the fracture (a measure of roughness and contact area of the fracture). The dotted curves reflect differing values of fracture compliance, α. Greater fracture compliance means that fracture apertures are more sensitive to changes in stress (increasing negative slopes in Figure 10). The squares are representative Marcellus samples. We delineate 3 regions: Fracture-Limited are fractures with such small values of N (effectively small hydraulic apertures) that stress changes do not significantly impact fracture permeability; Matrix-Limited are fractures that have such large values of N that the fractures always retain significant permeability and thus are not strongly affected by pressure drawdown; and Stress-Sensitive are fractures with combinations of fracture compliance α and N such that they are responsive to pressure drawdown. We further delineate Extreme to Low Significance for the effects of pressure drawdown. From Li et al. (2021b).

As an example application of the principles illustrated in Figure 11, we examine the effects of pressure drawdown for a stress-sensitive shale specimen in Figure 12. The results are shown in terms of the bottomhole pressure maintained during production. A very low bottomhole pressure is typical industry practice and will maximize production in the short term. However, by the 6-year mark, the practice of pressure management by maintaining relatively high bottomhole pressure (near 20 MPa) begin to show gains over typical practices. By 10 years, pressure management is clearly superior for these type of shales with a more than 20% increase in cumulative gas production.

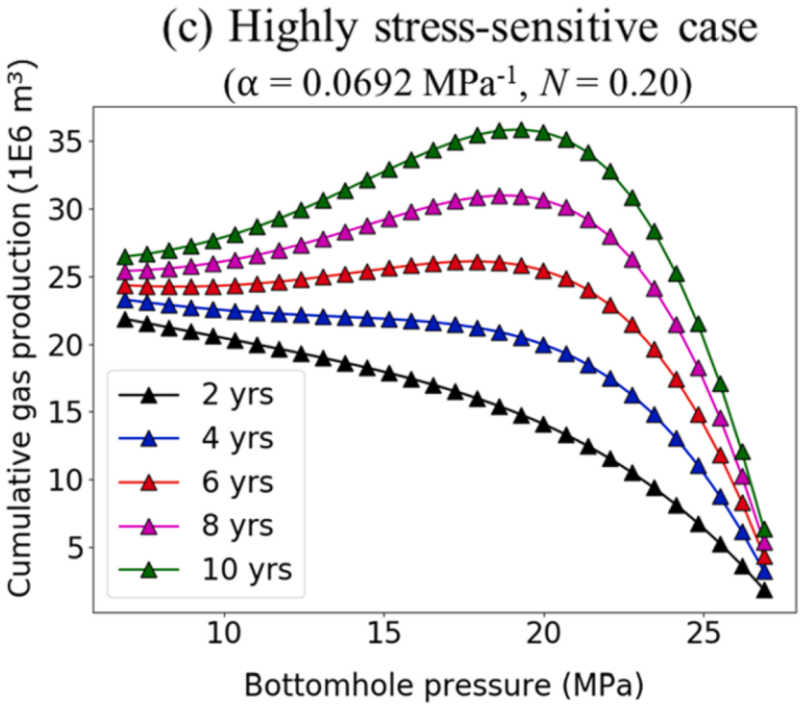

Figure 12. Calculated effects of managing bottomhole pressure (i.e., pressure drawdown management) on cumulative gas production as a function of production time. Low bottomhole pressures are equivalent to opening production valves completely (i.e., no pressure management). Optimal production can be obtained by maintaining a bottomhole pressure near 20 MPa. From Li et al. (2021b).

As a further application of these results, we examine the impact of varying the orientation of the well to take advantage of natural fractures. Here the objective is to place the primary hydraulic fractures such that they create the largest tributary fracture zone. The default orientation of the horizontal portion of an unconventional well is parallel to the minimum stress direction. However, this direction may not be optimal for engaging the existing natural fracture network. In Figure 13, we use discrete fracture network modeling to show that small changes (10^{o}) in the orientation can incorporate a greater extent of the natural fracture network and thereby increase cumulative production by up to 9%. This effect is independent of pressure management, but pressure management can further amplify the benefits of this strategy.

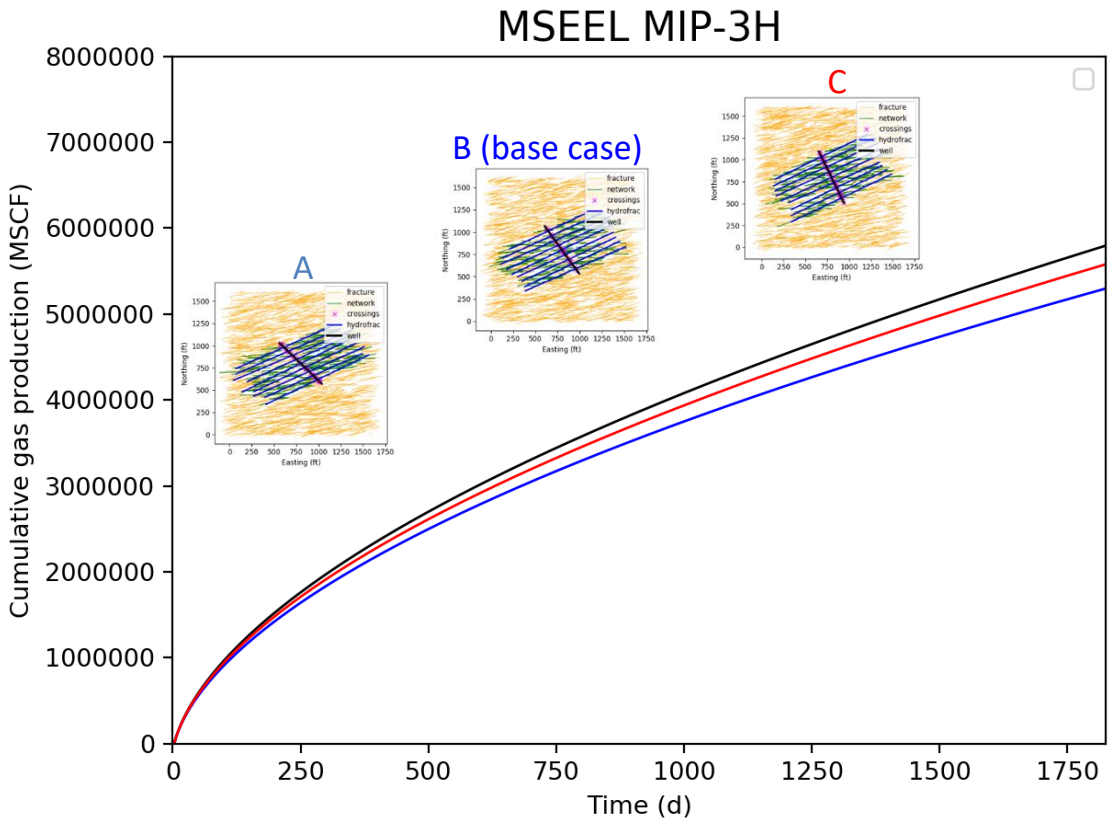

Figure 13. Computational analysis of the effect of well orientation on cumulative hydrocarbon production given interaction with a natural fracture network. This discrete fracture network calculation is based on the distribution and orientation of natural fractures at the MSEEL site. The base case is the traditional well orientation parallel the minimum horizontal stress. Cases A and C are oriented ±10^{o} from the base case. Both of the alternative orientations improve on the base case.

3.1. Enhanced Recovery from Unconventional Shale using CO_2

Traditional CO_2 Enhanced Oil Recovery (CO_2-EOR) techniques have been optimized and tested for conventional reservoirs. These techniques provide pressure maintenance to avoid multiphase conditions, improve the sweep efficiency and modify the hydrocarbon phase properties to improve fluid mobility. However, shale characteristics significantly affect these techniques and require optimizing these techniques for shale reservoirs. For instance, waterflooding, which is the most common EOR technique in conventional reservoirs, is not practical for shale reservoirs, mostly because of the ultra-low permeability shale formation and the impracticality of the multi-well EOR operations. On the other hand, the gas injection, and CO_2 injection particularly, has become a promising EOR technique for shale reservoirs.

To gain more insight, we compared the potential of carbon dioxide and nitrogen to improve hydrocarbon recovery using huff and puff operations (Nguyen et al., 2018). We used microfluidics techniques in which we created a synthetic fracture network filled with oil, which we subsequently pressurized with CO_2 or N_2. We observed that carbon dioxide yields higher recovery than nitrogen

for both connected and dead-end fractures and that connected fractures usually have a better recovery than dead-end ones for both gases as shown in Figure 14. We attribute this behavior to the superior miscibility characteristics of carbon dioxide.

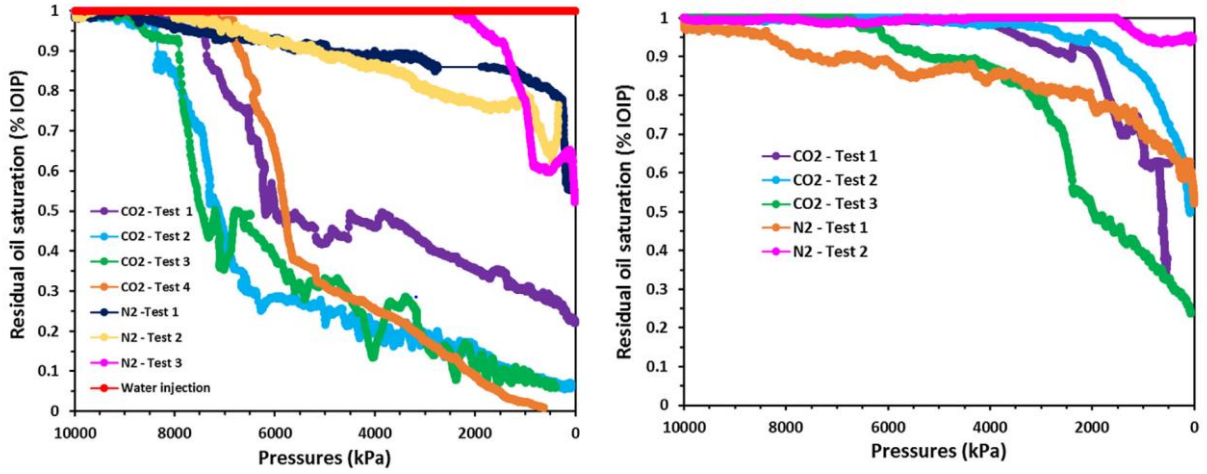

Figure 14. Residual oil saturation after huff and buff microfluidic experiments using carbon dioxide and nitrogen: connected fractures (left) and dead-end fractures (right). The experiments were repeated multiple times to evaluate reproducibility (Nguyen et al., 2018).

We used molecular simulations to further study carbon dioxide, nitrogen, and methane's capacity to extract hydrocarbons from rough organic pores (Mehana et al., 2020b). We found that confinement enhances hydrocarbons adsorption to the pore surface, hindering hydrocarbon mobility. We observed recovery factors up to 90% for concurrent displacements and recovery factors less than 20% for counter-current displacements. Notably, we found that the limited diffusion and miscibility of nitrogen in hydrocarbons led to faster recovery. In addition, methane yielded better recovery for counter-current displacement. However, carbon dioxide provides the best candidate as long as miscibility is achieved, as shown in Figure 15.

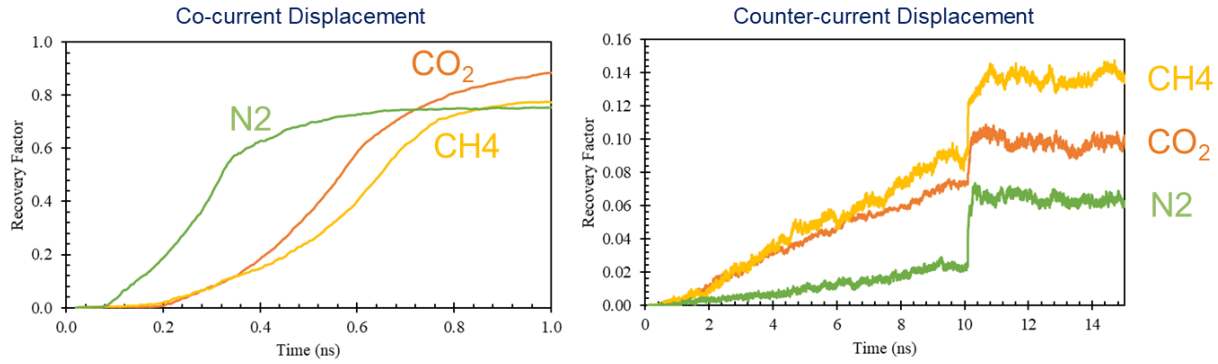

Figure 15. Molecular simulations predictions of the efficiency of carbon dioxide, methane, and nitrogen to extract hydrocarbons from organic pores. Co-current displacement involves an injection inlet for the gas and a production outlet for the hydrocarbon. In contrast, counter-current displacement, which is similar to huff and puff operations, involves injecting the gas and producing the hydrocarbons from the same port (adapted from Mehana et al. (2020b).

3.2. Key Take-aways from Tributary Fracture Zone (TFZ) Research

1. Developed a new experimental approach to determine TFZ production
2. We determined conditions that promote fracture branching and greater penetration of the unconventional shale matrix (Li et al., 2021a).
3. We conducted an extensive analysis of hydro-mechanical response of Marcellus shale (Li et al. 2021b).
4. We quantified the impact of fracture activation on enhanced fracture transmissivity (Welch et al. 2022).
5. We quantified the impact of resource depth on potential production (Frash et al. 2017).
6. We demonstrated how pressure drawdown can enhance production (Li et al. 2021b).
7. We developed theoretical foundation for pressure drawdown analysis (Li et al. 2021b).
8. We demonstrated a method for optimizing well orientation to enhance production.
9. We analyzed huff and puff strategies for enhancing hydrocarbon production from unconventional shale (Nguyen et al. 2018; Mehana et al. 2020b).

3.3. Next Steps for TFZ research

This research led to a contract with an oil and gas company to further develop the experimental approaches and concepts related to the tributary fracture zone. The next steps in further developing this approach include the following:

1. Understand and optimize fracture-matrix communication: there physical aspects of damage to the fracture wall (skin formation) and chemical aspects of hydraulic fracturing fluids damaging or blocking hydrocarbon migration pathways from matrix to fracture.
2. Self-propping of fractures: we have not yet addressed the longevity of the enhanced permeability we observed in tributary fracture zone experiments. Further studies comparing self-propping of shear fractures with propped hydraulic fractures would provide useful insights into fracture behavior.
3. Optimize fracture branching: include anisotropic stress conditions and other factors in relation to greater penetration of the hydraulic fracture system).

4. Hydraulic Fracture System

In our conceptual model, the large hydraulic fracture system operates at the reservoir scale and controls early production. Mid to late production is controlled by the tributary fracture zone and matrix processes described in sections 2 and 3, respectively. We developed LANL software dfnWorks (Hyman et al., 2015) partially under the fundamental shale program to mechanistically simulate the hydraulic fracture system, tributary fracture zone and matrix processes. dfnWorks has allowed us to determine the dominant mechanisms that control production at each scale and to explore pressure management scenarios that can be used to optimize production from unconventionals.

dfnWorks was developed to simulate reservoirs where flow and transport are fracture dominated. Figure 16 shows an example of a dfnWorks simulation with a horizontal well, hydraulic fractures and an array of natural background fractures. The hydraulic fractures intersect natural fractures, expanding the extent of the reservoir contributing hydrocarbon to the well. We used this type of simulation to simulate hydrocarbon production from unconventional reservoirs. In order to incorporate the contributions from the tributary fracture zone and matrix processes, we developed

additional model functionality that allowed us to represent the elevated permeability of the TFZ and the slower diffusive transport of hydrocarbon from matrix to the TFZ and primary hydraulic fractures.

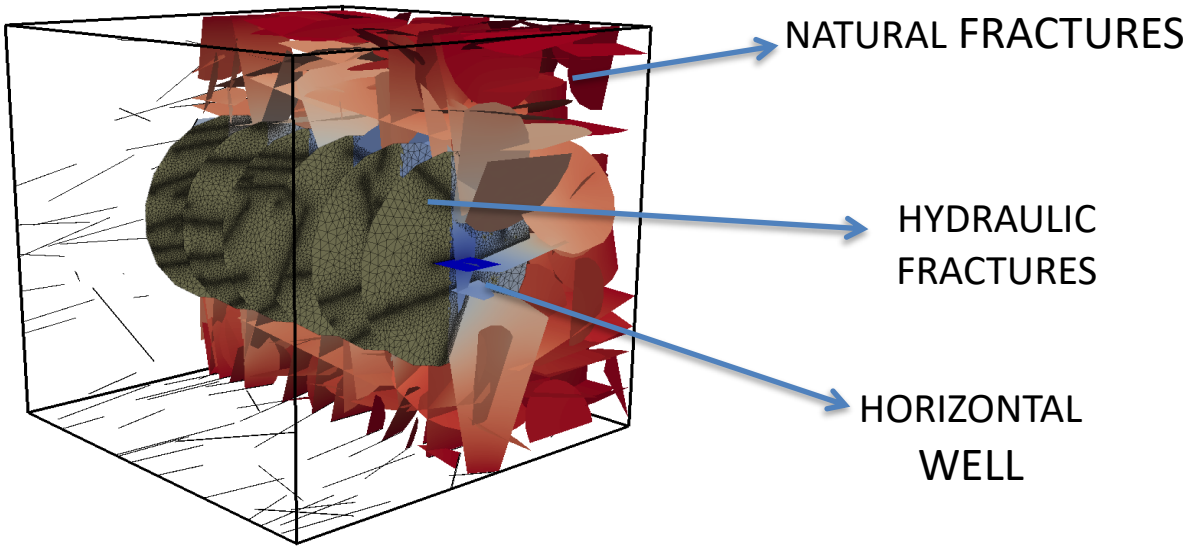

Figure 16: dfnWorks simulation of unconventional reservoir production. A horizontal well with hydraulic fractures emerging at six perforations that intersect pre-existing natural fractures.

Our discrete fracture simulations revealed the initial peak and early (< 1 year) production arises from drainage of high-permeability, large hydraulic and natural fractures. The connection of hydraulic fractures to an extended large-scale natural fracture allows continued but declining production. We observed later time (> 2 years) production that constitutes 80% of total hydrocarbon resource requires engagement of smaller-scale features: tributary fracture zone (Section 3) and ultimately the matrix (Section 4) (Figure 17).

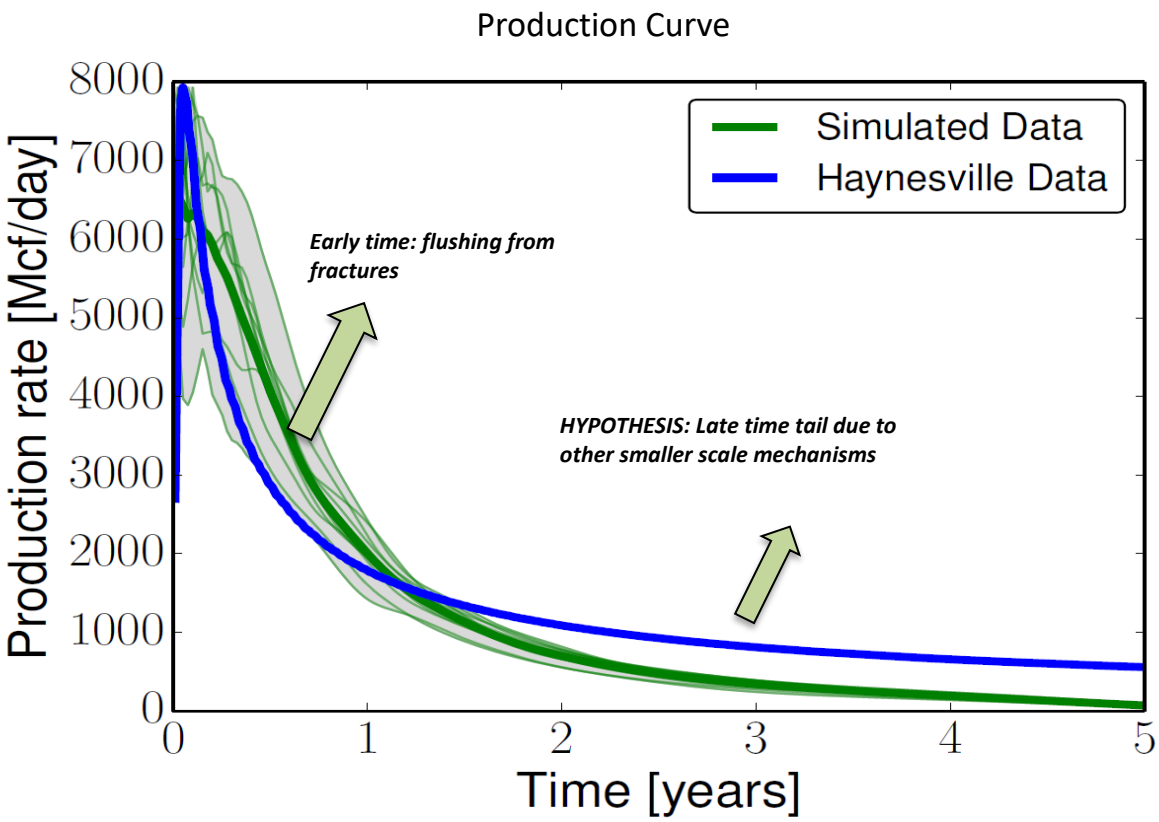

Figure 17: Unconventional reservoir production curve derived from Haynesville data showing early production controlled by rapid depletion of hydrocarbon from large hydraulic fracture and late-time production tailing controlled by the tributary fracture zone and matrix processes.

Using dfnWorks, Hyman et al. (2015) simulated a shale's production profile's main characteristics where they observed an initial peak followed by a steep decline (Figure 18, left). They matched features enabling advective transport. They intentionally did not include the matrix diffusion and other small-scale processes that might explain the observed mismatch during the later time of the well life. When the matrix diffusion was considered, better results were reported for the production tail (Karra et al., 2015). They suggested that other matrix processes are responsible for the remaining mismatch during the late production.

In the same vein, Lovell et al. (2018) refuted the perceived notion of the matrix diffusion effect on the production from shale reservoirs, as shown in Figure 18 (center). Instead, they demonstrated that matrix diffusion in the region of the fractured zone significantly impacts production from the first year. Interestingly, they also found that the depth of the fractured region did not affect the production curves' shape. However, the total mass of the hydrocarbon produced increases with the depth.

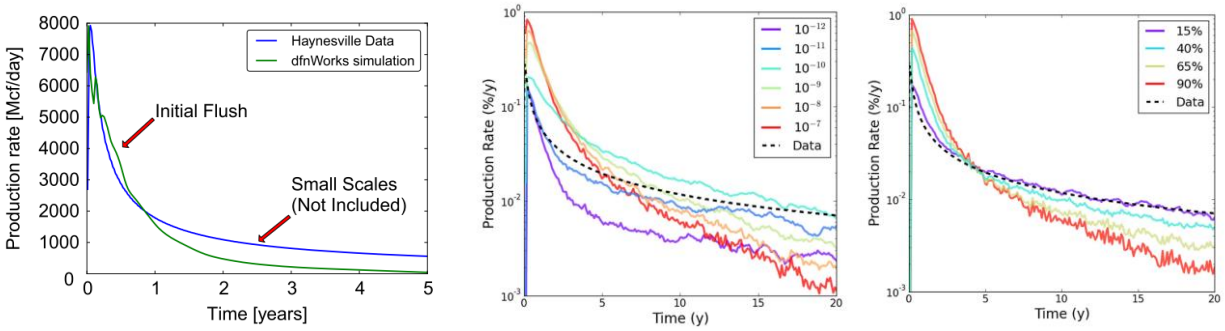

Figure 18. dfnWorks Monte Carlo predictions of well performance: A) highlighting the need to include the advective transport in the smaller fracture and the diffusion from the matrix to properly model the production tail (Hyman et al., 2015); b) highlighting the impact of diffusion coefficient on the production curve (Lovell et al., 2018); c) highlighting the effect of the percentage of free hydrocarbon outside the fractured zone on the production curve.

Investigating another mysterious subsurface phenomenon, our team integrated a DFN model with statistical analysis to reveal the fate of fracturing fluids (O'Malley et al. 2016). Although the fracturing operations require a large volume of fracturing fluid, less than half of these fluids flow back. They showed that most of the missing water (about 90%) resides in the matrix with a lesser amount in the fractures (about 10%). However, shale's ultra-low permeability nature makes it challenging to explain how these fluids could be transported and trapped in the matrix. Noting that shale gas reservoirs are naturally in a water under-saturated state, O'Malley et al. suggested that capillary forces are a significant driver for water imbibition into the ultra-tight shale matrix. This has implications for storing fluids such as CO_2 at unconventional sites that could lower the environmental footprint while increasing ultimate recovery. In addition, it could be a driver for a CO_2 economy in future climate-constrained scenarios.

We also explored an alternative mechanism for trapping injected fracturing fluids by osmosis as into the matrix (Mehana and El-Monier 2015). The salinity contrast between the fracturing fluid and the formation brine induces a pressure gradient. Mehana and El-Monier found that the osmotic pressure might be responsible for driving up to 50% of the fracturing fluid into the matrix.

The entrapment of fracturing fluids in the matrix would likely affect both the well performance and life. Firstly, these fluids would affect the hydrocarbon mobility near the wellbore. Consequently, it reduces the ultimate recovery of the well. Secondly, the fluid/rock interactions affect the petrophysical properties and strength of the rock. We found a relationship between the impact of the trapped fluids on the formation strength with the formation mineralogy (Mehana et al., 2018). Unlike the common belief, the formation strength is enhanced if it has more than 8% siderite and anhydrite content. However, the bottom line is the impact of these trapped fluids is adverse to hydrocarbon recovery. Therefore, LANL has pioneered the search for alternative environmental-friendly fracturing fluids, such as CO_2.

We described the use of supercritical carbon dioxide as a non-aqueous fracturing fluids that reduces the environmental footprint and simultaneously enhances hydrocarbon recovery (Middleton et al., 2014). We summarized the main merits of carbon dioxide, including superior adsorption, hydrocarbon mobility enhancement, and sequestration benefits (Middleton et al. 2015).

Recently, experimental investigations have quantified the benefits of using CO_2 as a fracturing fluid supporting our studies. Zhang et al. (2017) observed a reduction in the fracturing pressure and an increase in the fracture network's complexity. Natural gas is critical for enabling more renewable penetration onto the grid since it can load balancing the grid against renewables such as solar and wind that are intermittent. As the world prepares for future energy and climate scenarios, unconventionals with CO_2 as a fracturing fluid and storage sink have the potential to play a large role in a new CO_2 economy.

Despite the unprecedented success of hydraulic fracturing in developing shale reservoirs, significant environmental concerns have been raised. While it is unlikely for hydraulic fractures to create fractures that connect drinking water with shale formations, it is still possible to create fractures that connect faults and natural fractures. However, the majority of the reported leaks are associated with wellbore integrity. Wellbore integrity is also a cause of fugitive methane leaks and could be one of the more straightforward ways to lower the carbon footprint of unconventional sites. On the other hand, the induced seismicity is mainly associated with wastewater disposal, where the pore pressure increases, reducing the effective stress and potentially reactivating faults. In addition, hydraulic fractures could directly intersect with the fault zone. While disposal regulations have eased the severity of induced seismicity consequences, current research devises innovative fracturing fluids and addresses wellbore integrity problems.

5. Machine Learning Analysis of Production

The fundamental shale program allowed LANL to begin utilizing machine learning techniques to improve unconventional reservoir simulation. This work has transitioned to DOE's SMART initiative, where real-time decision making and forecasting continues to be developed. Here we describe our initial work under the fundamental shale program and some of the synergistic programmatic efforts occurring under SMART and internal LANL LDRD funding. Recent developments in machine learning have transformed the efficiency of many processes, but has lagged in impacting subsurface operations, particularly for unconventional reservoirs. This delay is mainly attributed to the limitations of sufficient subsurface data on these systems. Machine learning techniques tend to require large amounts of data. Therefore, this effort focused on devising physics-informed machine learning approaches that require less observational data. We also use standard machine learning efforts to analyze large databases of wells to determine trends and critical mechanisms. Fracture networks impart a higher degree of site-specificity in reservoir properties relative to conventional reservoirs, and the properties are often less well defined. Figure 19 outlines the main LANL applications of machine learning to accelerate and improve current subsurface models.

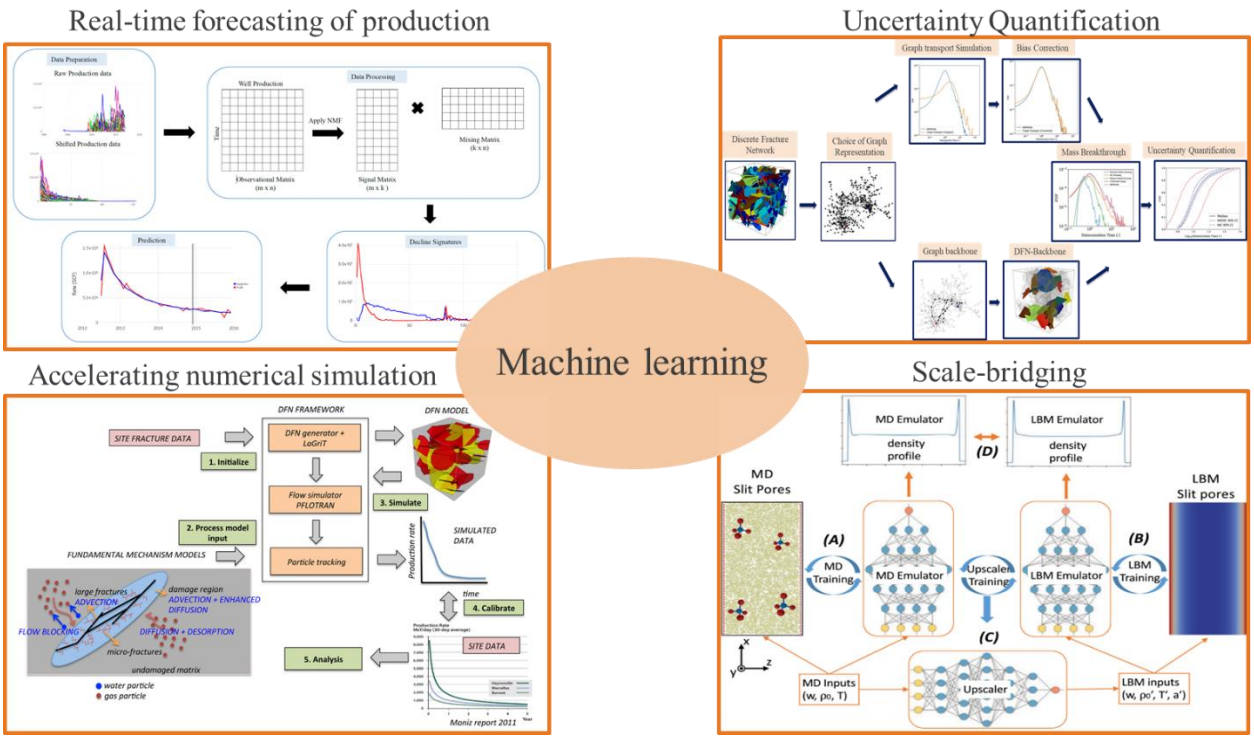

Figure 19. A summary of LANL's main applications of machine learning for subsurface modeling, including well performance predictions, uncertainty quantification, accelerating numerical simulations, and bridging the scales between molecular and pore scales.

A promising ML-based approach is to develop scale-bridging schemes to connect the atomistic-scale simulations with the pore- and reservoir-scale simulations. We proposed one of these scale-bridging schemes (Lubbers et al., 2020), which relies on deep learning techniques to quantify the adsorption characteristics in silt pores and inform LBM simulations. Essentially, we trained neural network simulators to predict the density profiles of the fluid at different conditions using molecular- and pore-scale simulation. Then, we trained another network to perform the upscaling. Apart from the computational speedup, we demonstrated the indirect coupling's applicability to scale the adsorption characteristics.

In the same vein, we adopted an active learning framework to accelerate neural network training. The approach we used sampled the parameter space efficiently to model the methane adsorption in complex pores using an active learning approach (Santos et al., 2020). We successfully reached the accuracy of conventional techniques using only 10% of the dataset. This work is the initial stage to develop a workflow to estimate the adsorption characteristics on the fly and inform LBM, enabling larger time and length scales. We further extended the work scope to model the transport properties using reinforcement learning (Wang et al., 2021). We used MD and LBM datasets to train physics-constrained neural networks.

The hydraulic fracturing success highly determines shale well performance since hydraulic fractures mechanically create conductive pathways connecting the natural fractures. Consequently, the production profile displays unique characteristics that differ from those observed in conventional reservoirs. The production rate quickly climbs to a peak, then gradually decreases with a long tail. Unlike the reservoir boundaries for conventional wells, the drainage area for a

shale well usually corresponds to the mechanically stimulated reservoir volume. The hydrocarbon's initial flush corresponds to the hydrocarbon residing in the hydraulic and natural fractures, marking the production history's linear flow portion. Unlike the conventional wells, the boundary-dominated flow does not usually follow the linear flow. However, intermediate flow regimes corresponding to the complexity of the fracture network are observed. These intermediate flow regimes are named tributary fracture depletion regimes. On the other hand, the long production tail usually accounts for the matrix phenomena such as desorption and diffusion.

Combining the extended linear flow and the indefinite onset of the boundary-dominated flow pose a challenge to the traditional forecasting approaches. In Mehana et al. (2020a), we adopted a Monte Carlo approach to predict shale reservoirs performance where mature well production characteristics predict newer well performance. In addition, we observed that 75% of the production history is required for the deterministic methods to provide reliable results. We used non-negative matrix factorization to extract the decline signature of shale well production profiles. These decline signatures were used to predict the well performance afterward. In addition, this approach provides early identification of underperforming wells.

Machine learning has been adopted to accelerate high-fidelity simulations of shale reservoirs. For this task, we used convolution neural networks to estimate effective diffusivity using the LBM dataset (Wu et al., 2019). Besides the computational efficiency of LBM, we achieved six orders of magnitude speedup. However, we observed poor performance for low-diffusivity pore structures, suggesting we should augment our approach with either multiscale feature extraction or geometrical properties to overcome this limitation. Similarly, using the LBM dataset, we also used a deep learning approach to predict the residual saturations during multiphase displacement in heterogeneous fractures (Guiltinan et al., 2020). We quantified the impact of the wettability heterogeneity on residual saturations. One limitation of commonly used ML architectures is that they cannot train with large domains ($>100^3$). Recently, we presented the MS-Net, a model that enables predictions up to 850^3 on a single GPU (Santos et al., 2021). We showcased the results by accurately predicting single-phase flow in single fractures and propped fractures.

Fluid transport in fractured reservoirs is a fundamental research challenge. While full-physics model predictivity has reached a reasonable degree of maturity, the computational cost is still a massive road blocker. In Srinivasan et al. (2018a), we proposed integrating graph theory and machine learning to accelerate the fractured media's high-fidelity simulations. We demonstrated that the graph representations require significantly lower degrees of freedom to model microstructures, leading to four orders of magnitude speedup. One of the challenging pieces of the puzzle for discrete fracture modeling is the computational expense. One promising technique to improve computational efficiency is system reduction, where machine-learning techniques are leveraged to identify the most significant fractures. LANL researchers pioneered backbone, connected sub-network, as a unit for classification instead of single fractures (Srinivasan et al., 2018b). In Srinivasan et al. (2019), we assessed the efficiency of using the random forest as a classification technique to identify the backbones for system reduction. We reported up to 90% of computational savings. We also highlighted the need for an efficient approach to generate the database required for training. We also examined the performance of logistic regression, where the reduced network could yield similar breakthrough curves similar to full-network ones (Srinivasan

et al., 2020). Figure 20 compares the computational intensity of dfnWorks and graph-based models for different fractured systems.

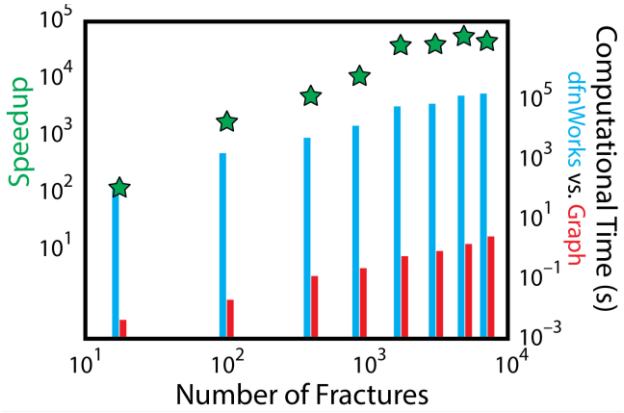

Figure 20. Comparison of computational speed for full-physics dfnWorks and the graph-based models trained from a suite of runs produced by dfnWorks. For large numbers of fractures, the graph-based models can be ~30,000 faster.

Conclusions

Energy security and independence are a top priority for any nation's existence. Technology advancements allowed the economic development of shale reservoirs as an energy resource. These reservoirs unique characteristics and challenging nature require an in-depth understanding of their properties to devise better strategies to improve recovery factors with minimal environmental footprints. In this work, we have worked collaboratively with members of the fundamental shale portfolio on tasks to optimize matrix processes, enhance production from small-scale (tributary) fracture zones, develop full-physics models of entire hydraulic fracture systems, and design machine-learning frameworks. We hope to continue advancing our fundamental understandings of these reservoirs and to devise innovative machine-learning frameworks to accelerate our high-fidelity simulation, bridge the scales, and reveal hidden features in our data. We plan to extend and further our projects to advance carbon dioxide utilization and sequestration in shale reservoirs in preparation for future energy and climate scenarios.

References

Alharthy, N., Teklu, T., Kazemi, H., Graves, R., Hawthorne, S., Braunberger, J., & Kurtoglu, B. (2015). *Enhanced oil recovery in liquid-rich shale reservoirs: laboratory to field.* Paper presented at the SPE annual technical conference and exhibition.

Ambrose, R. J., Hartman, R. C., Diaz Campos, M., Akkutlu, I. Y., & Sondergeld, C. (2010). *New pore-scale considerations for shale gas in place calculations.* Paper presented at the SPE unconventional gas conference.

Bažant, Z. P., Salviato, M., Chau, V. T., Viswanathan, H., & Zubelewicz, A. (2014). Why fracking works. *Journal of Applied Mechanics, 81*(10).

Carey, J. W., Frash, L., Ickes, T., & Viswanathan, H. S. (2017). *Stress Cycling and Fracture Permeability of Utica Shale using Triaxial Direct-Shear with X-ray Tomography.* Paper presented at the 51st US Rock Mechanics/Geomechanics Symposium.

Carey, J. W., Lei, Z., Rougier, E., Mori, H., & Viswanathan, H. (2015). Fracture-permeability behavior of shale. *Journal of unconventional oil and gas resources, 11*, 27-43.

Chen, L., Kang, Q., Dai, Z., Viswanathan, H. S., & Tao, W. (2015a). Permeability prediction of shale matrix reconstructed using the elementary building block model. *Fuel, 160*, 346-356.

Chen, L., Zhang, L., Kang, Q., Viswanathan, H. S., Yao, J., & Tao, W. (2015b). Nanoscale simulation of shale transport properties using the lattice Boltzmann method: permeability and diffusivity. *Scientific Reports, 5*(1), 1-8.

Chermak, J. A., & Schreiber, M. E. (2014). Mineralogy and trace element geochemistry of gas shales in the United States: Environmental implications. *International Journal of Coal Geology, 126*, 32-44.

Clarkson, C. R., Solano, N., Bustin, R. M., Bustin, A., Chalmers, G., He, L., . . . Blach, T. P. (2013). Pore structure characterization of North American shale gas reservoirs using USANS/SANS, gas adsorption, and mercury intrusion. *Fuel, 103*, 606-616.

Curtis, M. E., Cardott, B. J., Sondergeld, C. H., & Rai, C. S. (2012). Development of organic porosity in the Woodford Shale with increasing thermal maturity. *International Journal of Coal Geology, 103*, 26-31.

Frash, L. P., Carey, J. W., Ickes, T., and Viswanathan, H. S. (2017). Caprock integrity susceptibility to permeable fracture creation. International Journal of Greenhouse Gas Control, 64:60 – 72.

Frash, L. P., Carey, J. W., Lei, Z., Rougier, E., Ickes, T., and Viswanathan, H. S. (2016). High-stress triaxial direct-shear fracturing of Utica shale and in situ x-ray microtomography with permeability measurement. Journal of Geophysical Research, 121:5493–5508.

Guiltinan, E., Santos, J. E., & Kang, Q. (2020). *Residual Saturation During Multiphase Displacement in Heterogeneous Fractures with Novel Deep Learning Prediction.* Paper presented at the Unconventional Resources Technology Conference, 20–22 July 2020.

Hjelm, R. P., Taylor, M. A., Frash, L. P., Hawley, M. E., Ding, M., Xu, H., . . . Dewers, T. (2018). Flow-through compression cell for small-angle and ultra-small-angle neutron scattering measurements. *Review of Scientific Instruments, 89*(5), 055115.

Hyman, J. D., Karra, S., Makedonska, N., Gable, C. W., Painter, S. L., & Viswanathan, H. S. (2015). dfnWorks: A discrete fracture network framework for modeling subsurface flow and transport. *Computers & Geosciences, 84*, 10-19.

Karra, S., Makedonska, N., Viswanathan, H. S., Painter, S. L., & Hyman, J. D. (2015). Effect of advective flow in fractures and matrix diffusion on natural gas production. *Water Resources Research, 51*(10), 8646-8657.

Li, W., Frash, L. P., Carey, J. W., Welch, N. J., Meng, M., Nguyen, H., Viswanathan, H. S., Rougier, E., Lei, Z., Rahimi-Aghdam, S., and Bažant, Z. P. (2021a). Injection parameters that promote branching of hydraulic cracks. Geophysical Research Letters, 48(12):e2021GL093321.

Li, W., Frash, L. P., Welch, N. J., Carey, J. W., Meng, M., and Wigand, M. (2021b). Stress-dependent fracture permeability measurements and implications for shale gas production. Fuel, 290:119984.

Liu, X., & Zhang, D. (2019). A review of phase behavior simulation of hydrocarbons in confined space: Implications for shale oil and shale gas. *Journal of Natural Gas Science and Engineering, 68*, 102901.

Lovell, A. E., Srinivasan, S., Karra, S., O'Malley, D., Makedonska, N., Viswanathan, H. S., . . . Frash, L. (2018). Extracting hydrocarbon from shale: An investigation of the factors that influence the decline and the tail of the production curve. *Water Resources Research, 54*(5), 3748-3757.

Lubbers, N., Agarwal, A., Chen, Y., Son, S., Mehana, M., Kang, Q., . . . Viswanathan, H. S. (2020). Modeling and scale-bridging using machine learning: nanoconfinement effects in porous media. *Scientific Reports, 10*(1), 1-13.

Mehana, M., Al Salman, M., & Fahes, M. (2018). Impact of salinity and mineralogy on slick water spontaneous imbibition and formation strength in shale. *Energy & Fuels, 32*(5), 5725-5735.

Mehana, M., Callard, J., Kang, Q., & Viswanathan, H. (2020a). Monte Carlo simulation and production analysis for ultimate recovery estimation of shale wells. *Journal of Natural Gas Science and Engineering, 83*, 103584.

Mehana, M., & El-Monier, I. (2015). Numerical investigation of the osmatic flow impact on the load recovery and early well performance. *Journal of Petroleum Engineering and Technology, 5*(03).

Mehana, M., & El-monier, I. (2016). Shale characteristics impact on Nuclear Magnetic Resonance (NMR) fluid typing methods and correlations. *Petroleum, 2*(2), 138-147.

Mehana, M., Guiltinan, E., Vesselinov, V., Middleton, R., Hyman, J. D., Kang, Q., & Viswanathan, H. (2021a). Machine-Learning Predictions of the Shale Wells' Performance. *Journal of Natural Gas Science and Engineering*, 103819.

Mehana, M., Kang, Q., Nasrabadi, H., & Viswanathan, H. (2021b). Molecular Modeling of Subsurface Phenomena Related to Petroleum Engineering. *Energy & Fuels*.

Mehana, M., Kang, Q., & Viswanathan, H. (2020b). Molecular-Scale Considerations of Enhanced Oil Recovery in Shale. *Energies, 13*(24), 6619.

Melikoglu, M. (2014). Shale gas: Analysis of its role in the global energy market. *Renewable and Sustainable Energy Reviews, 37*, 460-468.

Middleton, R., Viswanathan, H., Currier, R., & Gupta, R. (2014). CO2 as a fracturing fluid: Potential for commercial-scale shale gas production and CO2 sequestration. *Energy Procedia, 63*, 7780-7784.

Middleton, R. S., Carey, J. W., Currier, R. P., Hyman, J. D., Kang, Q., Karra, S., . . . Viswanathan, H. S. (2015). Shale gas and non-aqueous fracturing fluids: Opportunities and challenges for supercritical CO2. *Applied Energy, 147*, 500-509.

Middleton, R. S., Gupta, R., Hyman, J. D., & Viswanathan, H. S. (2017). The shale gas revolution: Barriers, sustainability, and emerging opportunities. *Applied Energy, 199*, 88-95.

Neil, C. W., Hjelm, R. P., Hawley, M. E., Watkins, E. B., Cockreham, C., Wu, D., . . . Xu, H. (2020a). Small-angle Neutron Scattering (SANS) Characterization of Clay-and Carbonate-rich Shale at Elevated Pressures. *Energy & Fuels, 34*(7), 8178-8185.

Neil, C. W., Mehana, M., Hjelm, R. P., Hawley, M. E., Watkins, E. B., Mao, Y., . . . Xu, H. (2020b). Reduced methane recovery at high pressure due to methane trapping in shale nanopores. *Communications Earth & Environment, 1*(1), 1-10.

Nguyen, P., Carey, J. W., Viswanathan, H. S., & Porter, M. (2018). Effectiveness of supercritical-CO2 and N2 huff-and-puff methods of enhanced oil recovery in shale fracture networks using microfluidic experiments. *Applied Energy, 230*, 160-174.

O'Malley, D., Karra, S., Currier, R. P., Makedonska, N., Hyman, J. D., & Viswanathan, H. S. (2016). Where does water go during hydraulic fracturing? *Groundwater, 54*(4), 488-497.

Perrin, J., & Geary, E. (2019). EIA adds new play production data to shale gas and tight oil reports. In.

Rahimi-Aghdam, S., Chau, V.-T., Lee, H., Nguyen, H., Li, W., Karra, S., . . . Bažant, Z. P. (2019). Branching of hydraulic cracks enabling permeability of gas or oil shale with closed natural fractures. *Proceedings of the National Academy of Sciences, 116*(5), 1532-1537.

Rickman, R., Mullen, M. J., Petre, J. E., Grieser, W. V., & Kundert, D. (2008). *A practical use of shale petrophysics for stimulation design optimization: All shale plays are not clones of the Barnett Shale.* Paper presented at the SPE annual technical conference and exhibition.

Riewchotisakul, S., & Akkutlu, I. Y. (2015). *Adsorption enhanced transport of hydrocarbons in organic nanopores.* Paper presented at the SPE annual technical conference and exhibition.

Ross, D. J., & Bustin, R. M. (2009). The importance of shale composition and pore structure upon gas storage potential of shale gas reservoirs. *Marine and petroleum Geology, 26*(6), 916-927.

Santos, J. E., Mehana, M., Wu, H., Prodanovic, M., Kang, Q., Lubbers, N., . . . Pyrcz, M. J. (2020). Modeling nanoconfinement effects using active learning. *The Journal of Physical Chemistry C, 124*(40), 22200-22211.

Santos, J. E., Yin, Y., Jo, H., Pan, W., Kang, Q., Viswanathan, H., Prodanovic, M., Pyrcz, M., Lubbers, N. (2021). Computationally Efficient Multiscale Neural Networks Applied to Fluid Flow in Complex 3D Porous Media. *Transport in Porous Media*.

Seales, M. B., Ertekin, T., & Yilin Wang, J. (2017). Recovery efficiency in hydraulically fractured shale gas reservoirs. *Journal of Energy Resources Technology, 139*(4).

Sondergeld, C. H., Newsham, K. E., Comisky, J. T., Rice, M. C., & Rai, C. S. (2010). *Petrophysical considerations in evaluating and producing shale gas resources.* Paper presented at the SPE unconventional gas conference.

Srinivasan, G., Hyman, J. D., Osthus, D. A., Moore, B. A., O'Malley, D., Karra, S., . . . Viswanathan, H. S. (2018a). Quantifying topological uncertainty in fractured systems using graph theory and machine learning. *Scientific Reports, 8*(1), 1-11.

Srinivasan, S., Cawi, E., Hyman, J., Osthus, D., Hagberg, A., Viswanathan, H., & Srinivasan, G. (2020). Physics-informed machine learning for backbone identification in discrete fracture networks. *Computational Geosciences*, 1-16.

Srinivasan, S., Hyman, J., Karra, S., O'Malley, D., Viswanathan, H., & Srinivasan, G. (2018b). Robust system size reduction of discrete fracture networks: A multi-fidelity method that preserves transport characteristics. *Computational Geosciences, 22*(6), 1515-1526.

Srinivasan, S., Karra, S., Hyman, J., Viswanathan, H., & Srinivasan, G. (2019). Model reduction for fractured porous media: a machine learning approach for identifying main flow pathways. *Computational Geosciences, 23*(3), 617-629.

Wang, J., Chen, L., Kang, Q., & Rahman, S. S. (2016). Apparent permeability prediction of organic shale with generalized lattice Boltzmann model considering surface diffusion effect. *Fuel, 181*, 478-490.

Wang, K., Yu Chen, Mohamed Mehana, Nicholas Lubbers, Kane C. Bennett, Qinjun Kang, . . . Germann, T. C. (2021). A physics-informed and hierarchically regularized data-driven model for predicting

fluid flow through porous media. *Journal of Computational Physics*.

Wu, H., Fang, W.-Z., Kang, Q., Tao, W.-Q., & Qiao, R. (2019). Predicting effective diffusivity of porous media from images by deep learning. *Scientific Reports, 9*(1), 1-12.

Xu, H. (2020). Probing nanopore structure and confined fluid behavior in shale matrix: A review on small-angle neutron scattering studies. *International Journal of Coal Geology, 217*, 103325.

Yang, Y., Wang, K., Zhang, L., Sun, H., Zhang, K., & Ma, J. (2019). Pore-scale simulation of shale oil flow based on pore network model. *Fuel, 251*, 683-692.

Yoon, H., & Dewers, T. A. (2013). Nanopore structures, statistically representative elementary volumes, and transport properties of chalk. *Geophysical Research Letters, 40*(16), 4294-4298.

Zhang, X., Wang, J., Gao, F., & Ju, Y. (2017). Impact of water, nitrogen and CO2 fracturing fluids on fracturing initiation pressure and flow pattern in anisotropic shale reservoirs. *Journal of Natural Gas Science and Engineering, 45*, 291-306.

Project Deliverables

ID	Task Description	Status
1.0	**Develop & calibrate a reservoir-scale simulation platform that captures transport in matrix & fractures**	Complete
1.1	Develop the initial application of dfnWorks to elucidate the impact of pressure-management on recovery relative to a prototypical shale reservoir	Complete
1.2	Develop a reduced-order model that can relate hydrocarbon production as a function of fracture-related parameters such as natural fracture density, hydraulic fracture size and number of stimulation stages	Complete
1.3	Develop a reduced-order model that relates production (and/or recovery efficiency) to pressure drawdown	Complete
2.0	**Determine experimentally the transport properties of fractures**	Complete
2.1	Determine transport behavior in fractures as a function of stress conditions, pressure drawdown, shale properties, etc	Complete
2.2	Develop microfluidics analysis of multiphase flow behavior for a suite of shale samples and fluid compositions to evaluate the impact on transport due	Complete

	to different fluids (e.g., CO2, H2O with surfactants, hydrocarbons) that could be used in secondary-recovery strategies	
3.0	**Determine based on experiments and theoretical simulations the fundamental transport phenomena in shale matrix**	Complete
3.1	Development of neutron experiments to quantify the fraction of closed pores in a range of shale samples. Will initially be calibrated to MSEEL-I.	Complete
3.2	Perform a physics-based analysis (based on lattice Boltzmann methods) to quantify the effects of pore-scale mineralogy and heterogeneity on apparent permeability, extending our initial results to a range of shale-matrix properties	Complete
3.3	Integration of pore-scale results into a revised set of parameters for dfnWorks . Will initially be calibrated to MSEEL-I.	Complete
4.0	**Identify opportunities for science-informed machine-learning for unconventional reservoirs**	Complete
4.1	Technical basis for opportunities in physics-informed machine learning in hydrocarbon recovery from unconventional reservoirs. This will feed Task 7 of the SMART initiative	Complete
4.2	Draft technical plan for the use of physics-informed machine learning to develop new solutions for improved efficiency and reliability in reservoir management for unconventional reservoirs. This will feed Task 7 of the SMART initiative	Complete